Data-association-free Characterization of Labeling Uncertainty: the Cross Modeling Tracker

CARLOS MORENO LEON
HANS DRIESSEN
ALEXANDER YAROVOY

The Multiple Object Tracking problem for a known and constant number of closely-spaced objects in a track-before-detect context is considered. The underlying problem of decomposing a data-association-free Bayes posterior density is analyzed. A previously proposed solution for two objects moving in one-dimensional space is generalized for higher dimensional problems where *t* objects move in a M-dimensional space. The underlying problem is solved with the proposed Cross Modeling Tracker by means of hypothesizing physical crosses between the objects for a general *t–MD* objects case. In particular, the mathematical definition of cross-between-objects is generalized from a meaningful interpretation of the problem in the low dimensional setting. A method to provide optimal references for evaluation of the Cross Modeling Tracker is also considered. The Cross Modeling Tracker algorithm is validated with the optimal references by simulating *t–MD* closely-spaced objects scenarios. Wider applicability of the Cross Modeling Tracker with respect to comparable reviewed solutions is demonstrated via simulation experiments.

Manuscript received February 17, 2021; revised July 7, 2021; released for publication December 1, 2021.

Associate Editor: Florian Meyer.

C.M. Leon is with Fraunhofer FHR - Cognitive Radar, Wachtberg, Germany (E-mail: carlos.moreno@fhr.fraunhofer.de).
H. Driessen and A.G. Yarovoy are with Delft University of Technology - Microwave Sensing, Signals and Systems, Delft, The Netherlands (E-mail: {J.N.Driessen, A.Yarovoy}@tudelft.nl)

NOMENCLATURE

MOT	Multiple Object Tracking.
DBT	Detect-before-track.
TBD	Track-before-detect.
RFS	Random Finite Sets.
SNR	Signal to Noise Ratio.
DA	Data-association.
CMT	Cross Modeling Tracker.
MMSE	Minimum Mean Square Error.
JPDA	Joint Probabilistic Data Association.
MHT	Multiple Hypothesis Tracking.
PHD	Probability Hypothesis Density.
LMB	Labeled Multi-Bernoulli.
GOSPA	Generalized Optimal Subpatern Assignment.
PF	Particle Filter.
LPE	Labeled Point Estimates.
MD	M-dimensional.
t	Number of objects.
$\boldsymbol{s}_k$	State vector at time k.
o_k	Variable "order" at time k.
$\boldsymbol{\varkappa}_k$	DBT measurement at time k with indication of correct data association.
$\boldsymbol{Z}_k$	Sequence of DBT measurements up to, and including, time k.
$\boldsymbol{z}_k$	DBT measurement at time k.
$\mathbf{Z}_k$	Sequence of complete TBD measurements up to, and including, time k.
$\mathbf{z}_k$	Complete TBD measurement at time k.
N_r, N_b	Number of range and bearing cells in $\mathbf{z}_k$.
$z_k^{i,j}$	TBD measurement at cell i, j.
N_p	Number of particles.

I. INTRODUCTION

Multiple Object Tracking (MOT) refers to the problem of jointly estimating the presence and states or trajectories of objects based on measurements from sensors such as radars. The majority of reported MOT solutions are only suitable in detect-before-track (DBT) context, i.e., designed for detection measurements. This paper aims to solve the MOT problem for a known and constant number of closely-spaced objects in a track-before-detect (TBD) context.

The problem of deciding which track state estimate belongs to which physical object over time is known as the labeling problem. Labels are considered as unique identifiers assigned to each physical object in the track initiation stage. In closely-spaced objects tracking, sensor systems may not provide enough information to uniquely match objects labels and objects point estimates consistently over time, leading to uncertainty in the labeling [3]. Labeling uncertainty can play a role already in sensor systems even if the objects can be

resolved by the sensor. This will occur if maneuverability of the objects and/or sensor update intervals get large.

The terms labeling problem and labeling uncertainty might be misleading, it is important to remark that there is no uncertainty in the labels as they have been assigned (and are therefore fully known) within the tracker. The uncertainty is about the assignment of tracks to the fully known set of labels [17]. However, due to historical reasons, we will continue referring to this problem and the uncertainty as labeling problem and labeling uncertainty.

Labels have been rigorously incorporated in MOT solutions by two different means. Firstly, by using random vector formulations. In this case, the order of partitions in the random vector implicitly determines the labels of the tracks. Secondly, by using random finite sets (RFS) formations and explicitly introducing labels as additional components in the (unordered) state variable. The scope of this paper is limited to the case of known and constant number of objects in order to isolate the essence of the labeling problem. Under this assumption, a vector formulation suffices.

TBD MOT uses multiple frames of the raw sensor measurements with the objective of avoiding a hard thresholding decision. Consequently, TBD algorithms jointly estimate the existence of the target (detection) as well as track its kinematic state (filtering).

Avoidance of hard thresholding in TBD prevents loss of information, which is remarkably important in the tracking of low signal to noise ratio (SNR) objects. Additionally, TBD MOT cope with closely-spaced objects tracking in cases where a DBT approach would have to deal with merged measurements. Therefore, TBD MOT provides an inherently increased resolution capability over DBT MOT, which however makes it all the more important to address data-association-free characterization of labeling uncertainty.

The advantages of TBD tracking motivate this paper to design an algorithm able to characterize labeling uncertainty without using data-association (DA) techniques. The aim of such algorithm is adding labeling characterization capabilities to regular TBD filters such as the one presented in [6]. The lack of practical solutions is discussed in the Literature Review section. In order to fill the gap, this paper generalizes the association-free framework in [17, Section IV] to arbitrarily high dimensional problems.

The paper is organized as follows. Section II presents the research questions and specifies the underlying problem to answer them. Also, an extensive literature review on the topic is provided. Section III presents a generic formulation to characterize the Cross Modeling Tracker (CMT). Section IV revisits the evaluation method specifically design in [18] to measure estimation performance of the CMT. Sections V and VI provide the analytical generalization of the method presented in [17, Section IV] to the general t–MD objects case. Simulation results are also provided. Section VII draws final conclusions and proposes future research directions.

II. PROBLEM DESCRIPTION AND CONTEXTUALIZATION IN LITERATURE

Consider an MOT problem based on raw (TBD) measurements and a scenario containing t objects moving in a M-dimensional space (t–MD setting). Additionally, consider that t is constant and known by the tracker.

In cases where the objects move far apart from each other, labeling uncertainty is negligible and a regular TBD tracker such as the one in [6] suffices to infer the correct pair-matching between labels and point estimates. However, when the t objects move closely-spaced, labeling uncertainty degrades tracking performance and even the optimal TBD MOT solution is prevented from inferring the correct pair-matching between labels and point estimates. It is important to remark that what we refer to as pair-matching between labels and point estimates is conceptually different from the well-studied pair-matching problem between detections and labels (detections do not even exist in TBD). This difference is described in Appendix A.

Precisely due to the mathematical limitations for providing uncertainty-free labeling in complicated scenarios, estimation of certainty regarding all potential labeling possibilities is a topic of major importance. For this reason, the problem considered in this paper is described by the following two questions:

- What is the list of $t!$ labeled point estimates for the current dynamic state of the objects? Here each labeled point estimate hypothesises the state of the t targets with indication of the labels.
- What is the certainty corresponding to each labeled point estimate in the list?

A regular TBD tracker is known to fail at answering these questions in closely-spaced objects scenarios for two reasons. First, particle-based approximations (required due to the highly non-linear nature of the TBD measurement models) cannot approximate multimodal densities for long periods of time [7]. This can be tackled by using a convenient proposal density [15]. Second, extraction of minimum mean square error (MMSE) point estimates from a TBD multimodal posterior density results in track-coalescence underperformance [5]. This can be solved efficiently by means of characterizing the labeling uncertainty implicitly contained in the TBD multimodal density [17]. The purpose of this paper is providing such characterization for the general t–MD objects case.

A. Formulation of the Problem

The link between the DA problem and the labeling problem is formulated mathematically in Appendix A. It

is concluded that in DBT context, the labeling problem is implicitly solved by tackling the DA problem. Unfortunately, the same analytic method cannot be applied in TBD filtering to solve the labeling problem due to the absence of detections.

In TBD context, $\mathbf{z}_k$ contains the power reflected from the tracking scenario for each radar cell at time step k. For instance, a 2D raw data set $\mathbf{z}_k$ can be modeled as in [6] by $N_r \times N_b$ power measurements z_k^{ij}, where $i = 1, 2, ..., N_r$ and $j = 1, 2, ..., N_b$.

The permutation of measurement $\boldsymbol{z}_k$ described in Appendix A makes no sense for the TBD measurements $\mathbf{z}_k$. Therefore $\pi_m(\mathbf{z}_k)$ (see Appendix A) cannot be used to hypothesize labeling associations in TBD. However, the decomposition using permutations in $\boldsymbol{s}_k$, derived in Appendix A, can be formulated also in TBD:

$$p(\boldsymbol{s}_k|\mathbf{Z}_k) \propto \sum_{m=1}^{t!} l(\mathbf{z}_k|\pi_m(\boldsymbol{s}_k))p(\boldsymbol{s}_k|\mathbf{Z}_{k-1}). \tag{1}$$

We consider the worst case scenario, where TBD measurements do not incorporate information about objects' labels. Under this assumption, the TBD likelihood model for the measurements conditioned on the state $l(\mathbf{z}_k|\boldsymbol{s}_k)$ is invariant with respect to permutation of partitions in the state vector:

$$l(\mathbf{z}_k|\pi_m(\boldsymbol{s}_k)) = l(\mathbf{z}_k|\pi_n(\boldsymbol{s}_k)) \quad \forall\{m, n\} : \{\pi_m, \pi_n\} \in \Pi. \tag{2}$$

This is a remarkable difference with respect to DBT, where $l(\boldsymbol{z}_k|\boldsymbol{s}_k)$ is permutation variant (even when the measurements do not provide any information about the labels). Due to equation (2), equation (1) provides a decomposition in which all components end up being identical disregarding whether objects are closely-spaced or not. For this reason, equation (1) is certainly not relevant for labeling characterization in TBD. In fact, it can be simplified as:

$$\begin{aligned} p(\boldsymbol{s}_k|\mathbf{Z}_k) &\propto \sum_{m=1}^{t!} l(\mathbf{z}_k|\pi_m(\boldsymbol{s}_k))p(\boldsymbol{s}_k|\mathbf{Z}_{k-1}) \\ &\propto l(\mathbf{z}_k|\boldsymbol{s}_k)p(\boldsymbol{s}_k|\mathbf{Z}_{k-1}). \end{aligned} \tag{3}$$

The simplification in equation (3) illustrates that, although $p(\boldsymbol{s}_k|\mathbf{Z}_k)$ can be calculated, an analytical decomposition of $p(\boldsymbol{s}_k|\mathbf{Z}_k)$ cannot be accessed by the TBD filter. This defines the specific problem which needs to be tackled to answer the two questions of interest.

B. Related Literature

A plethora of MOT techniques have been developed over recent decades including Joint Probabilistic Data Association (JPDA) [13], Multiple Hypothesis Tracking (MHT) [21], and Probability Hypothesis Density (PHD) [19]. These algorithms are designed to work with detections. As the scope of this paper is within TBD MOT, none of these methods are suitable.

Some RFS-based trackers use multitrajectory densities instead of multiobject densities [23]. A multitrajectory random variable incorporates the states of the entire history for each trajectory in the set. With this information, track formation is enabled without any type of label incorporation. Although some reported RFS multitrajectory trackers accommodate TBD models [16], answering the two questions in the Problem Description section does not require information about the entire history of the trajectories.

In [14], an RFS-based mutiobject filter is adapted to work in TBD context. The adaptation is based on fitting a particle-based multiobject density approximation as a Labeled Multi-Bernoulli (LMB) RFS density after each filtering iteration. Nonetheless, questions in the Problem Description section cannot be answered. In fact, the so-called Improved LMB filter provides low Generalized Optimal Subpatern Assignment (GOSPA) errors at the expense of losing labeling information.

In [24], a backward simulation method is proposed to recover full trajectory (labeling) information from unlabeled filtering mutiobject densities. However, the process (generating unlabeled filtering posteriors, recovering trajectory information and marginalizing to obtain the filtering density of interest) involves unnecessary complexity overhead. This is specially so in TBD context, where RFS prior conjugacy cannot be exploited as particle-based approximations are required to accommodate highly nonlinear measurement models. Additionally, the problem in the scope of this paper does not even need to be formulated with RFS as the number of objects is assumed known and constant.

Aoki et al. provided a mathematical characterization of the labeling uncertainties with clear physical interpretation in [1]. However, the proposed Multitarget Sequential Monte Carlo filter algorithm involves a computational complexity of $O(N_p^2 t!^2)$. This computational bottleneck is prohibitive for tracking scenarios with more than two objects.

Blom and Bloem [4] introduced a decomposition of the exact Bayes posterior density into the weighted sum of permutation invariant and permutation strictly variant components. The so-called "unique decomposition" was used by García-Fernández in [15] to provide a particle filtering solution relevant for our problem description. The main focus in [15] is on calculating the probability of successful labeling after object separation, where the posterior multiobject density has symmetric nature [8], [20]. In particular, the contribution of García-Fernández to the characterization of labeling uncertainty problem is based on linking the so-called probability of successful labeling to the particular metric and point estimate considered [15]. These contributions where exemplified for the tracking of two objects with wireless sensor networks.

A generalization of the "unique decomposition" [4] was provided by Croise et al. in [9], where the main focus is to demonstrate how this decomposition can be used to

approximate Minimum Mean Optimal Subpartern Assignment (MMOSPA) estimates . Although MMOSPA estimates do not provide answers to the questions in the Problem Description section due to its unlabeled nature, it is important to remark that the consideration of Optimal Subpartern Assignment (OSPA) metric (or its generalization GOSPA) has been reported successful at preventing track-coalescence. However, MMOSPA estimates are very computationally demanding to calculate and therefore its implementation in dynamic systems has only been reported under some approximations [10], [11].

The use of MMOSPA estimates has been encouraged by the majority of reviewed solutions. Only [15] has reported successful results at avoiding track-coalescence using MMSE estimates. This becomes possible as the specific problem formulated in Section II-A is tackled by incorporating characterization of labeling uncertainty in the filtering process. Interestingly, this characterization does not rely on DA techniques and therefore it is usable in TBD. Unfortunately, although proposed as future work in [15], the generalization of this solution for more than two objects has not been addressed.

An alternative solution for incorporating DA-free characterization of labeling uncertainty in the filtering process was provided in [17, Section IV]. Although this solution tackles the problem formulated in Section II-A, it is only usable for the 2–1D objects case. Specifically, the generalization of [17, Section IV] is the gap to be filled with the contribution in this paper.

C. Detailed Review of [17, Section IV]: Modeling Crosses for the 2–1D Objects Case

Fig. 1 illustrates the idea of *cross modeling* in the most simple scenario where the labeling problem appears: two one-dimensional objects approach each other, stay closely-spaced for a while and finally split.

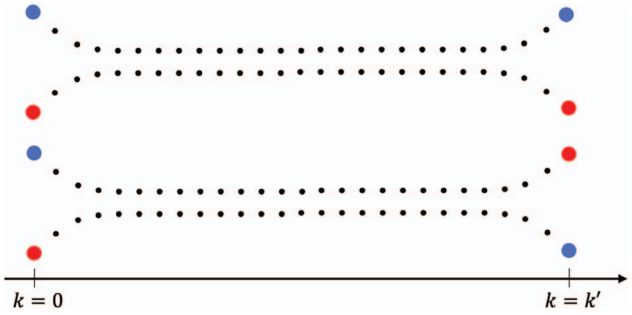

Fig. 1. Representation on top hypothesizes that objects have (physically) crossed an even number of times from $k = 0$ to $k = k'$. Representation at the bottom hypothesizes that objects have (physically) crossed an odd number of times from $k = 0$ to $k = k'$.

At $k = 0$, the tracker places a label to each object according to the tracker's convention: e.g., blue to the target that is further away and red to the other. At any later point in time, for instance $k = k'$, two labeling possibilities are worth considering. One where the furthest object is blue and the nearest one red (example trajectories on top of the figure) and the other with opposite colors, positions being the same (example trajectories at the bottom of the figure).

Note that the questions in Section II do not ask about past states but only current information, for instance at $k = k'$. However, although full trajectory information is not required, it is essential to estimate whether the objects have crossed an even or an odd number of times from $k = 0$ to $k = k'$ in order to characterize the two possible labeling solutions.

Based on described estimation of crosses, [17, Section IV] proposed a method to decompose the association-free TBD multiobject posterior density. For closely-spaced objects situations, the non-decomposed $p(\boldsymbol{s}_k|\mathbf{Z}_k)$ in equation (3) displays symmetric multimodality:

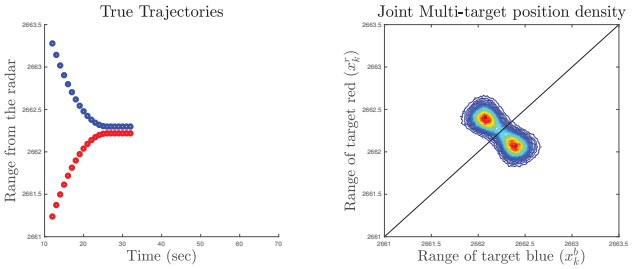

Fig. 2. Illustration of a closely-spaced targets situation. Ground truth trajectories of two targets moving in a line (2–1D objects scenario) in the left-hand side. Last joint multiobject position density (position components of $p(\boldsymbol{s}_k|\mathbf{Z}_k)$) represented in the right-hand side.

One interpretation of the multimodality in $p(\boldsymbol{s}_k|\mathbf{Z}_k)$ with physical meaning is that the objects may have well crossed each other from one time scan to the next one. As one can see in Fig. 2, the probability mass of $p(\boldsymbol{s}_k|\mathbf{Z}_k)$ concentrates in separated regions of the joint state space. These regions represent different labeling permutations of the information of interest.

In [17, Section IV], it is assumed that the state variable is a vector where partitions are stacked: $\boldsymbol{s}_k = [x_k^b\ \dot{x}_k^b\ x_k^r\ \dot{x}_k^r]^T$. Positions of each partition are denoted as x_k and velocities as $\dot{x}_k$. b and r are the labels for the first and second partition respectively (blue and red for printing clarity). In order to hypothesize crosses between objects, the concept of *order* at time step k was defined in [17, Section IV] as:

$$o_k = d(\boldsymbol{s}_k) = \begin{cases} 1 \text{ if } x_k^b > x_k^r \\ 2 \text{ otherwise.} \end{cases} \tag{4}$$

For two objects moving in one dimension, the variable *order* determines whether the position of one 1D object is larger or less than the position of another 1D object. Also, it is trivial to interpret a permutation of *order* in the state vector as a cross of objects between time steps $k-1$ and k:

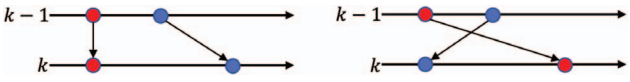

Fig. 3. No permutation of *order* (left-hand side), permutation of *order* (right-hand side).

The notion of order/cross escapes to physical interpretation in higher dimensional problems. One cannot tell whether the position of one 2D object is larger or less than the position of another 2D object as the definition of ">" and "<" is only valid in the 1D line. In fact, although one *order* definition was provided in [17, Section V] for the 2–2*D* objects case, counterexamples were found proving it wrong.

III. GENERALIZED CHARACTERIZATION OF CROSS MODELING

Fig. 4 illustrates the block diagram of the CMT algorithm required to solve the formulated problem in Section II-A:

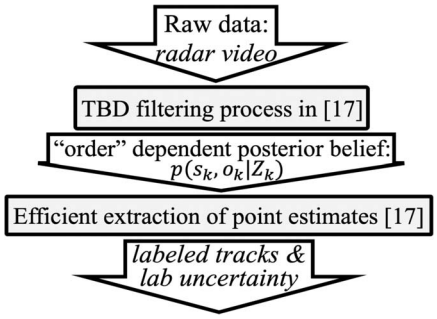

Fig. 4. This TBD framework was pictured in an equivalent way in [17]. Although the block diagram of the algorithm is generic, the definition of o_k in [17, Section IV] does not allow its use out of the 2–1*D* objects case. Hence, the importance of generalizing the definition of o_k.

The solution to be generalized ([17, Section IV]) was designed for particle-based implementations of the Bayesian filter. In particle filtering, "particle mixing" is a characteristic phenomenon inherent in approximations of multimodal densities [12]. Interestingly for our labeling problem, when "particle mixing" happens at least two particles are represented with permuted order of partitions in the state vector [8]. In order to generalize the definition of order/cross in [17, Section IV] to arbitrarily high dimensional problems, this paper proposes to analyze and exploit "particle mixing" effects in the particle cloud. Exploitation of such "particle mixing" analysis is realized by means of clustering the particle cloud.

Clustering the particle cloud results in remarkable benefits compared to existent methods. These benefits are: straightforward extraction of labeling certainty measures and trouble-free use of computationally efficient MMSE estimation (even when $p(\boldsymbol{s}_k|\mathbf{Z}_k)$ is multimodal).

A. State Space Model

The general nonlinear dynamic system and observation models can be denoted as f and q respectively:

$$\boldsymbol{s}_k = f(\boldsymbol{s}_{k-1}, \boldsymbol{n}_{k-1}), \tag{5}$$

$$\mathbf{z}_k = q(\boldsymbol{s}_k, \boldsymbol{v}_k),\ k \in \mathbb{N}, \tag{6}$$

where $\boldsymbol{s}_k, \boldsymbol{n}_k, \mathbf{z}_k$, and $\boldsymbol{v}_k$ represent the state, process noise, measurement, and measurement noise, respectively.

We tackle the MOT problem in the framework of recursive Bayesian filtering. The predicted and posterior densities of interest $p(\boldsymbol{s}_k|\mathbf{Z}_{k-1})$ and $p(\boldsymbol{s}_k|\mathbf{Z}_k)$ are obtained by iteration over the Chapman–Kolmogórov and Bayes equations:

$$p(\boldsymbol{s}_k|\mathbf{Z}_{k-1}) = \int p(\boldsymbol{s}_k|\boldsymbol{s}_{k-1})p(\boldsymbol{s}_{k-1}|\mathbf{Z}_{k-1})d\boldsymbol{s}_{k-1}, \tag{7}$$

$$p(\boldsymbol{s}_k|\mathbf{Z}_k) = \frac{p(\mathbf{z}_k|\boldsymbol{s}_k)p(\boldsymbol{s}_k|\mathbf{Z}_{k-1})}{p(\mathbf{z}_k|\mathbf{Z}_{k-1})}, \tag{8}$$

in this framework, the models in equations (5) and (6) are expressed in the form of $p(\boldsymbol{s}_k|\boldsymbol{s}_{k-1})$ and $p(\mathbf{z}_k|\boldsymbol{s}_k)$, respectively.

Due to the nonlinear nature of TBD measurement models, the Bayesian recursion formulated in equations (7) and (8) cannot be implemented via (stochastic) parametric models [22]. For this reason, a particle filter (PF) will be used to approximate the recursion.

B. A Generic Decomposition of $p(\boldsymbol{s}_k|\mathbf{Z}_k)$ in TBD

As detailed in the Section II-A, the underlying concern to answer the questions in Section II is how to decompose $p(\boldsymbol{s}_k|\mathbf{Z}_k)$ in TBD. A generic decomposition of $p(\boldsymbol{s}_k|\mathbf{Z}_k)$ can be formulated by introducing an auxiliary variable o_k:

$$p(\boldsymbol{s}_k|\mathbf{Z}_k) = \sum_{i=1}^{t!} p(\boldsymbol{s}_k, o_k = i|\mathbf{Z}_k). \tag{9}$$

Please note that the desired definition of o_k is not the one in equation (4) as we are targeting its generalization to the *t–MD* objects case. The new density of interest $p(\boldsymbol{s}_k, o_k|\mathbf{Z}_k)$, can be factorized as:

$$p(\boldsymbol{s}_k, o_k|\mathbf{Z}_k) = p(\boldsymbol{s}_k|o_k, \mathbf{Z}_k)P(o_k|\mathbf{Z}_k), \tag{10}$$

where $p(\boldsymbol{s}_k|o_k, \mathbf{Z}_k)$ is the posterior density of the state vector given o_k and the measurements, while $P(o_k|\mathbf{Z}_k)$ is the posterior probability of o_k. Both can be computed using the association-free (non-decomposed) TBD filter output $p(\boldsymbol{s}_k|\mathbf{Z}_k)$ and a certain probabilistic definition of the auxiliary variable o_k:

$$p(\boldsymbol{s}_k|o_k, \mathbf{Z}_k) = \frac{P(o_k|\boldsymbol{s}_k, \mathbf{Z}_k)p(\boldsymbol{s}_k|\mathbf{Z}_k)}{P(o_k|\mathbf{Z}_k)}, \tag{11}$$

$$P(o_k|\mathbf{Z}_k) = \int_{\boldsymbol{s}_k} P(o_k|\boldsymbol{s}_k)p(\boldsymbol{s}_k|\mathbf{Z}_k)d\boldsymbol{s}_k. \tag{12}$$

Assuming that the generalized definition of o_k is conditionally independent on $\mathbf{Z}_k$ given $\boldsymbol{s}_k$ (this is the case for the solution in [17, Section IV]), equation (11) can be rewritten as:

$$p(\boldsymbol{s}_k|o_k,\mathbf{Z}_k)=\frac{P(o_k|\boldsymbol{s}_k)p(\boldsymbol{s}_k|\mathbf{Z}_k)}{P(o_k|\mathbf{Z}_k)}. \tag{13}$$

The generic decomposition in equation (9) together with the desired statistical definition of order $P(o_k|\boldsymbol{s}_k)$ should allow answering the questions of interest. When MMSE estimation is the choice for extracting point estimates, the desired definition $P(o_k|\boldsymbol{s}_k)$ should ensure that each component in equation (9) $p(\boldsymbol{s}_k|o_k = m,\mathbf{Z}_k)$ is unimodal. Under this condition, the list of $t!$ label point estimates (question 1) can be provided avoiding track-coalescence. Finally, the desired definition $P(o_k|\boldsymbol{s}_k)$ should be such that $P(o_k = m|\mathbf{Z}_k)$ represent the certainty of labeling association m (question 2).

1) Labeled Point Estimates and Labeling Certainties of the CMT: In a particle-based implementation of the Bayesian recursion, $p(\boldsymbol{s}_k|\mathbf{Z}_k)$ is represented with a weighted set of particles $\{\boldsymbol{s}_k^i, w_k^i\}_{i=1}^{N_p}$. According to the decomposition in equation (9), MMSE order-dependent labeled point estimates (LPEs) can be calculated as the expected value of $\boldsymbol{s}_k$ given the *order* and measurements:

$$\begin{aligned}E[\boldsymbol{s}_k|o_k,\mathbf{Z}_k]&=\int_{\boldsymbol{s}_k}\boldsymbol{s}_k p(\boldsymbol{s}_k|o_k,\mathbf{Z}_k)d\boldsymbol{s}_k\\ &\underset{\text{Eq(13)}}{=}\frac{1}{P(o_k|\mathbf{Z}_k)}\int_{\boldsymbol{s}_k}\boldsymbol{s}_k P(o_k|\boldsymbol{s}_k)p(\boldsymbol{s}_k|\mathbf{Z}_k)d\boldsymbol{s}_k\\ &\approx\frac{1}{P(o_k|\mathbf{Z}_k)}\sum_i w_k^i\boldsymbol{s}_k^i P(o_k|\boldsymbol{s}_k^i).\end{aligned} \tag{14}$$

Order-dependent labeling certainties are necessarily in the second factor of equation (10):

$$P(o_k|\mathbf{Z}_k)=\int_{\boldsymbol{s}_k}P(o_k|\boldsymbol{s}_k)p(\boldsymbol{s}_k|\mathbf{Z}_k)d\boldsymbol{s}_k\approx\sum_i w_k^i P(o_k|\boldsymbol{s}_k^i). \tag{15}$$

Evaluation of $E[\boldsymbol{s}_k|o_k,\mathbf{Z}_k]$ for each possible realization of o_k provides a different vector of LPEs (answer to question 1):

$$\begin{aligned}E[\boldsymbol{s}_k|o_k=m,\mathbf{Z}_k]&\approx\frac{1}{P(o_k=m|\mathbf{Z}_k)}\sum_i w_k^i\boldsymbol{s}_k^i P(o_k=m|\boldsymbol{s}_k^i)\\ &\approx\frac{1}{P(o_k=m|\mathbf{Z}_k)}\sum_{i|o_k^i=m}w_k^i\boldsymbol{s}_k^i\ \text{ where } m\in\{1,2,..,t!\}.\end{aligned} \tag{16}$$

In the same way, evaluation of $P(o_k|\mathbf{Z}_k)$ for each possible realization of o_k provides a scalar with the associated labeling probability (answer to question 2):

$$P(o_k=m|\mathbf{Z}_k)\approx\sum_i w_k^i P(o_k=m|\boldsymbol{s}_k^i)\approx\sum_{i|o_k^i=m}w_k^i. \tag{17}$$

2) Algorithm Implementation: Alg. 1 is the practical implementation of the functionalities illustrated in Fig. 4.

ALGORITHM 1 Pseudo-code of the PF algorithm for implementation of the CMT. Extensions over the plain SIR TBD particle filter plus traditional MMSE estimate extraction are highlighted in blue color. $p(\boldsymbol{s}_k)$ and $p(\boldsymbol{n}_k)$ denote the initial prior and the process noise models.

$k=0$
Draw N_p samples $\boldsymbol{s}_k^i$ from $p(\boldsymbol{s}_k)$
Draw N_p samples $\boldsymbol{n}_k^i$ from $p(\boldsymbol{n}_k)$
$k=k+1$
$\boldsymbol{s}_k^i=f(\boldsymbol{s}_{k-1}^i,\boldsymbol{n}_{k-1}^i)$
Calculate o_k^i according to the definition of "order" under test
Given $\mathbf{z}_k$, obtain $\tilde{w}_k^i=p(\mathbf{z}_k|\boldsymbol{s}_k^i)$
Normalize weights $w_k^i=\tilde{w}_k^i/\sum_{j=1}^{N_p}\tilde{w}_k^j$
Resample from $\hat{p}(\boldsymbol{s}_k|\mathbf{Z}_k)=\sum_{i=1}^{N_p}w_k^i\delta(\boldsymbol{s}_k-\boldsymbol{s}_k^i)$:
Extract LPEs according to equation (16)
Obtain certainty measures of LPEs according to equation (17)
go to 3

IV. PERFORMANCE EVALUATION OF THE CROSS MODELING (CM) METHOD

Before delving into the main contribution of this paper, this section provides an optimal reference for future evaluation of the generalized CMT. Also, the validation of the solution in [17, Section IV] is provided in this section. Two algorithms implementing the optimal reference were provided in [18] based on the link between the DA problem and the labeling problem. In order to provide a self-contained explanation, the essential theory required to build up the optimal references is provided in Appendix A. The method we apply to validate the CMT can be summarized as follows:

In DBT context and taking the considerations from the sixth bullet point in Appendix A.

- Generate the analytical decomposition of $p(\boldsymbol{s}_k|\mathbf{Z}_k)$:

$$p(\boldsymbol{s}_k|\mathbf{Z}_k)\propto\sum_{m=1}^{t!}l(\pi_m(\boldsymbol{z}_k)|\boldsymbol{s}_k)p(\boldsymbol{s}_k|\mathbf{Z}_{k-1}). \tag{18}$$

- For each data-association-dependent component $l(\pi_m(\boldsymbol{z}_k)|\boldsymbol{s}_k)p(\boldsymbol{s}_k|\mathbf{Z}_{k-1})$
  - Extract MMSE labeled point estimates (optimal reference):

$$\begin{aligned}&E[p(\pi_m(\boldsymbol{z}_k)|\boldsymbol{s}_k)p(\boldsymbol{s}_k|\mathbf{Z}_{k-1})]\\ &=\int_{\boldsymbol{s}_k}\boldsymbol{s}_k p(\pi_m(\boldsymbol{z}_k)|\boldsymbol{s}_k)p(\boldsymbol{s}_k|\mathbf{Z}_{k-1})d\boldsymbol{s}_k.\end{aligned} \tag{19}$$

– Extract labeling certainty associated (optimal reference):

$$p(\pi_m(\boldsymbol{z}_k)|\boldsymbol{Z}_k) = \frac{\int l(\pi_m(\boldsymbol{z}_k)|\boldsymbol{s}_k)p(\boldsymbol{s}_k|\boldsymbol{Z}_{k-1})d\boldsymbol{s}_k}{\sum_{m=1}^{t!}\int l(\pi_m(\boldsymbol{z}_k)|\boldsymbol{s}_k)p(\boldsymbol{s}_k|\boldsymbol{Z}_{k-1})d\boldsymbol{s}_k}. \tag{20}$$

- Decompose $p(\boldsymbol{s}_k|\boldsymbol{Z}_k)$ from equation (18) using the CMT decomposition (equation (9)):

$$p(\boldsymbol{s}_k|\boldsymbol{Z}_k) = \sum_{m=1}^{t!} p(\boldsymbol{s}_k, o_k = m|\boldsymbol{Z}_k). \tag{21}$$

- For each data-association-free component $p(\boldsymbol{s}_k, o_k = m|\boldsymbol{Z}_k)$, factorize it as in equation (10) and:
  – Extract CMT MMSE labeled point estimates according to equation (16).
  – Extract CMT labeling certainty associated according to equation (17).

It is very important to remark that, although the CMT is motivated by the needs of TBD filtering, performance of the CMT can only be evaluated in the context of DBT. This becomes apparent when considering the evaluation method described above this lines. Please note that the optimal references in equations (19) and (20) need to be derived from the DBT analytical expression in equation (18). Nonetheless, the validation in DBT guaranties equivalent estimation performance of the CMT in TBD. This is because the CMT is designed to infer the relevant DA-free decomposition of any posterior density, disregarding whether it (the posterior density) was generated in the context of DBT or TBD.

Estimation performance of the CMT can be measured as the quality of the decomposition in equation (21). This is done in following sections by using the results in equations (19) and (20) as the optimal reference to answer the questions in Section II. For the validation of the proposed generalization of "order," the results in equations (16) and (17) will be compared with the optimal reference.

A. Algorithm Implementation

Alg. 2 implements the generation of the optimal references to answer questions in Section II based on the decomposition of equation (18). Concerning the second Remark in the Appendix A, $p(\boldsymbol{s}_k|\boldsymbol{Z}_{k-1})$ is commonly formulated as a mixture of densities in algorithms such as MHT, leading to exponentially increasing number of hypotheses over time. However, in the context of this paper, equation (18) is implemented with a single particle filter. Therefore, $p(\boldsymbol{s}_k|\boldsymbol{Z}_{k-1})$ can be formulated as a single density, even when it has multimodal nature.

ALGORITHM 2 Pseudo-code for generation of optimal references (lines 9 and 10) to answer questions in Section II.

1 $k = 0$
2 Draw N_p samples $\boldsymbol{s}_k^j$ from $p(\boldsymbol{s}_k)$
3 Draw N_p samples $\boldsymbol{n}_k^j$ from $p(\boldsymbol{n}_k)$
4 $k = k + 1$
5 $\boldsymbol{s}_k^j = f(\boldsymbol{s}_{k-1}^j, \boldsymbol{n}_{k-1}^j)$
Generate data-association-dependent posterior beliefs
6 for i=1 until t!
7 Given $\boldsymbol{z}_k$, obtain $\tilde{w}_k^{i,j} = p(\pi_i(\boldsymbol{z}_k)|\boldsymbol{s}_k^j)$
8 Normalize weights $w_k^{i,j} = \tilde{w}_k^{i,j} / \sum_{j=1}^{N_p} \tilde{w}_k^{i,j}$
9 Extract LPEs according to the particle – based approximation of equation (19)
10 Obtain certainty measures of LPEs according to particle – based approximation of equation (20)
Sum data-association-dependent posteriors in order to approximate $p(\boldsymbol{s}_k|\boldsymbol{Z}_k)$ with a single particle cloud
11 for j=1 until N_p
12 $w_k'^j = \sum_{i=1}^{t!} w_k^{i,j}$
13 Normalize weights $w_k^j = w_k'^j / \sum_{j=1}^{N_p} w_k'^j$
14 Resample N_p times from $\hat{p}(\boldsymbol{s}_k|\boldsymbol{Z}_k) = \sum_{j=1}^{N_p} w_k^j \delta(\boldsymbol{s}_k - \boldsymbol{s}_k^j)$ to generate $\hat{p}(\boldsymbol{s}_k|\boldsymbol{Z}_k) = \frac{1}{N_p}\sum_{j=1}^{N_p} \delta(\boldsymbol{s}_k - \boldsymbol{s}_k^j)$
go to 3

B. Performance Evaluation of [17, Section IV]

The choice of simulation parameters to evaluate the solution in [17, Section IV] is shown in Table I. This parametrization generates high amount of labeling uncertainty in order to challenge the MOT algorithm. This becomes apparent when considering the overlapping in between partitions of different colors (labels) of the predicted and posterior particle cloud in Fig. 5.

The evaluation can be reproduced by setting up the trajectories for the objects with initial and minimum distance as indicated by d_i and d_m in Table I. The evaluation considers the dynamic and measurement models as nearly constant velocity [2] and linear-Gaussian. The standard deviations of the process noise and observation noise are indicated by σ_n and σ_v, respectively, in Table I,

TABLE I
Parameters of the simulation

Parameter	Value
d_i	1.66 m
d_m	0.22 m
σ_n	0.14 m/s$^{3/2}$
σ_v	0.045 m
τ	1 s
N_p	10000 particles

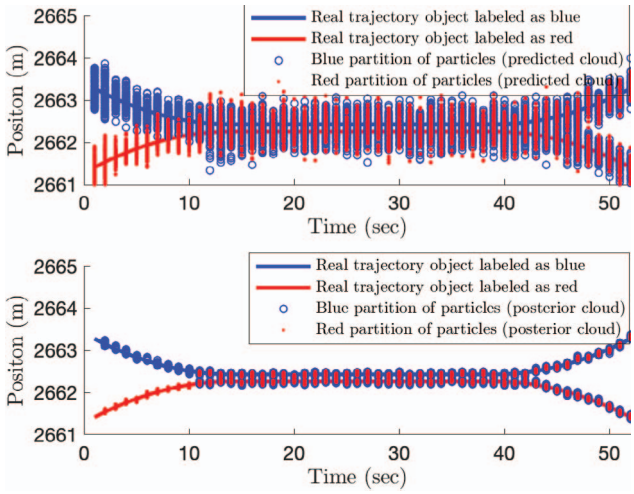

Fig. 5. Illustration of real trajectories as well as predicted and posterior particle clouds along all simulation time steps. The particle mixing effect can be observed, for instance, in the posterior particle clouds after object separation. In fact, different particles hypothesize the state of the same physical object with different partitions.

where τ denotes the revisit time. Without loss of generality, choosing these simple models suffices to validate Alg. 1 with Alg. 2.

The definition of o_k in equation (4) can be rewritten in a probabilistic form:

$$\begin{aligned} P(o_k = 1|\boldsymbol{s}_k) &= 1 \;\; if \;\; x_k^b > x_k^r, \\ P(o_k = 2|\boldsymbol{s}_k) &= 1 \;\; if \;\; x_k^b \leq x_k^r. \end{aligned} \tag{22}$$

The definition in equation (22) can be plugged into equations (13) and (12) in order to decompose $p(\boldsymbol{s}_k|\boldsymbol{Z}_k)$ using the CMT (Alg. 1). By these means, LPEs and associated labeling certainties can be generated with Alg. 1 and evaluated with the optimal reference generated by Alg. 2. Simulation results illustrated in Figs. 6 and 7 validate the cross modeling solution for the 2–1D objects case using the evaluation method described along this section.

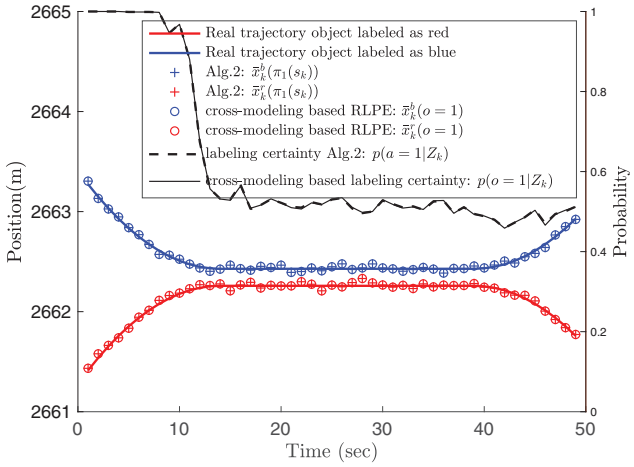

Fig. 6. Evaluation of estimation performance of the CM method for a 2–1D objects scenario. Cross modeling based estimates are extracted only from the cluster associated to "order" 1.

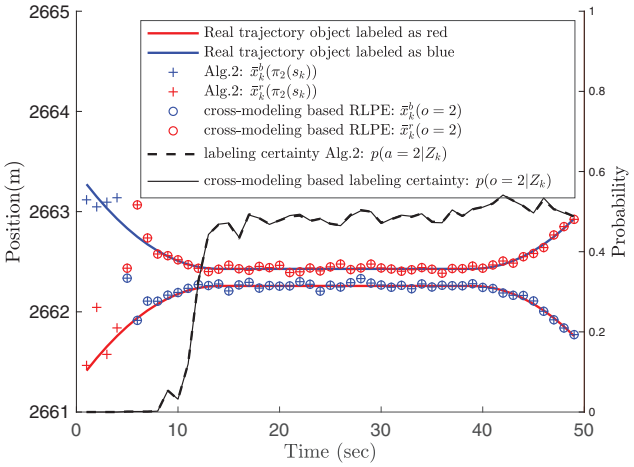

Fig. 7. Evaluation of estimation performance of the CM method for a 2–1D objects scenario. Cross modeling based estimates are extracted only from the cluster associated to "order" 2.

1) Comments on the Results: Alg. 1 decomposes the particle cloud in two ($t!$) clusters. These clusters explicitly approximate the DA-free decomposition in equation (9). The cluster associated to "order" 1 supports the hypothesis that the maneuvers of the two labeled objects lead to non-crossed trajectories with respect to the initialization $\forall k$. This cluster produces LPEs represented in Fig. 6 as $\bar{x}_k^{b,r}(o=1)$. The certainty measure associated ($P(o=1|\boldsymbol{Z}_k)$ curve) is extracted from the particle approximation of the joint multiobject posterior in step 11 of Alg. 1.

Over the first 4 seconds of the simulation, the LPE($o=1$) holds full certainty. No single particle belongs to the cluster $o=2$ and therefore, no representative can be extracted from there (see Fig. 7). As expected, $P(o_k=1|\boldsymbol{Z}_k)$ drops down to around 0.5 after the objects remain closely-spaced for some time. This means that labeling information has been completely lost. Labeling information cannot be recovered after the split as suggested by the measure of certainty. The LPE($o=2$) supports the hypothesis that the maneuvers of the two labeled objects lead to crossed trajectories with respect to the initialization $\forall k$.

Estimation results produced by the CMT closely match the optimal references generated by Alg. 2. This validates the CM method as a solution to the problem defined in the Section II-A for the 2–1D objects scenario.

V. FIRST GENERALIZATION OF THE DEFINITION OF *cross*: SCENARIOS WITH ARBITRARY NUMBER t OF 1D OBJECTS

For 2–1D object settings, equation (4) provides the *order* of any particle given its state. We will refer to this calculation as an absolute evaluation of *order*. Unlike 1-D points, 2-D points cannot be ordered making use of

the operators $\leq$ and $>$. For this reason, finding an absolute evaluation of "order" in 2-D is not a trivial concern.

A. Absolute Versus Relative *Order* Calculation and the Definition of *Cross*:

An alternative method to obtain the *order* can be realized by relative evaluation: relying on the prior *order* at time step $k-1$ and detecting whether or not the objects have crossed from time step $k-1$ to k,

	$P(o_k = 1\|\boldsymbol{s}_k) = 1$	$P(o_k = 2\|\boldsymbol{s}_k) = 1$
$P(o_{k-1} = 1\|\boldsymbol{s}_{k-1}) = 1$	no cross	cross
$P(o_{k-1} = 2\|\boldsymbol{s}_{k-1}) = 1$	cross	no cross

For 2–1D objects scenarios:

	$x_k^r < x_k^b$	$x_k^r \geq x_k^b$
$x_{k-1}^r < x_{k-1}^b$	no cross	cross
$x_{k-1}^r \geq x_{k-1}^b$	cross	no cross

Therefore, for a cross to be declared, one of the two following conditions should hold:

$$x_{k-r}^r < x_{k-r}^b \quad and \quad x_k^r \geq x_k^b, \tag{23}$$

$$x_{k-r}^r \geq x_{k-r}^b \quad and \quad x_k^r < x_k^b. \tag{24}$$

The relative "order" evaluation method shifts the generalization problem from the definition of *order* to the definition of *cross*. A *cross* detector for 2–1D objects can be derived from the absolute definition in equation (4). Let us denote $\boldsymbol{s}_k'^p$ as the position part of the state vector $\boldsymbol{s}_k = [x_k^b\ \dot{x}_k^b\ x_k^r\ \dot{x}_k^r]$ of particle p at time step k: $\boldsymbol{s}_k'^p = [x_k^{p,b}\ x_k^{p,r}]$. Since $\boldsymbol{s}_k'^p$ and $\boldsymbol{s}_{k-1}'^p$ are vectors in a 2D space (two objects placed along 1D spacial dimension), one can calculate the Euclidean distance or $l2-norm$ between them in the joint space as (superscript p is dropped for notation simplicity):

$$norm(\boldsymbol{s}_k' - \boldsymbol{s}_{k-1}') = \sqrt{(x_k^r - x_{k-1}^r)^2 + (x_k^b - x_{k-1}^b)^2} \tag{25}$$

$$= \sqrt{(x_k^r)^2 - 2(x_k^r x_{k-1}^r) + (x_{k-1}^r)^2 + (x_k^b)^2 - 2(x_k^b x_{k-1}^b) + (x_{k-1}^b)^2} \tag{26}$$

$$= \sqrt{(x_k^b - x_{k-1}^r)^2 + (x_k^r - x_{k-1}^b)^2 + 2(x_{k-1}^r - x_{k-1}^b)(x_k^b - x_k^r)} \tag{27}$$

Then,

$$norm^2(\boldsymbol{s}_k' - \boldsymbol{s}_{k-1}') = (x_k^b - x_{k-1}^r)^2 + (x_k^r - x_{k-1}^b)^2 + 2(x_{k-1}^r - x_{k-1}^b)(x_k^b - x_k^r) \tag{28}$$

$$norm^2(\boldsymbol{s}_k' - \boldsymbol{s}_{k-1}') = norm^2(\Pi\boldsymbol{s}_k' - \boldsymbol{s}_{k-1}') + K \tag{29}$$

where $K = 2(x_{k-1}^r - x_{k-1}^b)(x_k^b - x_k^r)$ and Π denotes the permutation matrix:

$$\Pi = \begin{pmatrix} 0 & 1 \\ 1 & 0 \end{pmatrix}. \tag{30}$$

Each of the equations (23) and (24) define conditions for a cross to be declared. Interestingly, when any of these equations is applied to function K, the result is $K > 0$ as long as $x_{k-1}^r, x_{k-1}^b, x_k^r$ and x_k^b take positive values. Variables $x_{k-1}^r, x_{k-1}^b, x_k^r$, and x_k^b can only take positive values in our application problem as these are range magnitudes. Therefore, inequation (31) holds as long as a cross in the state vector of particle p takes place:

$$norm^2(\boldsymbol{s}_k'^p - \boldsymbol{s}_{k-1}'^p) \ > \ norm^2(\Pi\boldsymbol{s}_k'^p - \boldsymbol{s}_{k-1}'^p). \tag{31}$$

Equivalently, the next *order switch* condition can be used to find out whether or not a cross should be declared for the particle p between time instants $k-1$ and k.

$$norm(\boldsymbol{s}_k'^p - \boldsymbol{s}_{k-1}'^p) \ > \ norm(\Pi\boldsymbol{s}_k'^p - \boldsymbol{s}_{k-1}'^p). \tag{32}$$

The result in equation (32) can be pictured in a physically meaningful way:

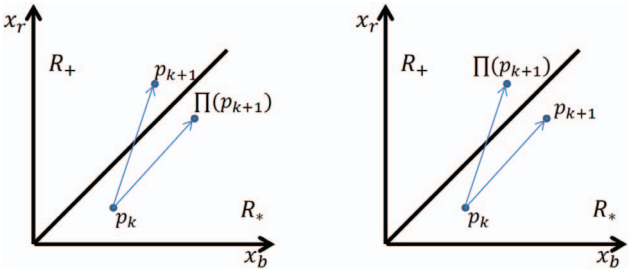

Fig. 8. The illustration in the left hand side represents an *order switch* as the points p_k and p_{k+1} belong to different sides of the diagonal $x_r = x_b$. Indeed, inequation (32) holds in this case. In the right hand side the point p does not cross the line $x_r = x_b$ between time instants k and $k+1$ meaning that the order remains the same in this case. Indeed, inequation (32) does not hold.

B. Generalization of *Cross* from 2–1D to t–1D Cases

This generalization considering 1D objects makes use of the relative definition of "order" based on inequation (32), applied to all possible pairs of partitions in the state vector. As the number of possible labeling solutions is $t!$, only the extension from two to three targets will be exemplified due to space limitations. Nevertheless, there is no loss of generality as the same technique can be applied to any arbitrary number of targets t.

For a three-object scenario, the three partitions in the state vector can be ordered in six different ways according to, for instance, the following convention:

TABLE II
As an example, this convention will group in cluster 1 those particles complying with: position of the first partition is less than the position of the second partition, being the position of the second partition less than the position of the third partition. For the sake of printing clarity in forthcoming simulation experiments, the first, second and third partitions will be identified with colors green, red, and blue, respectively.

	1D magnitude increasing direction →
$o=1$	$1^{st}\ 2^{nd}\ 3^{rd}$
$o=2$	$1^{st}\ 3^{rd}\ 2^{nd}$
$o=3$	$2^{nd}\ 1^{st}\ 3^{rd}$
$o=4$	$3^{rd}\ 1^{st}\ 2^{nd}$
$o=5$	$2^{nd}\ 3^{rd}\ 1^{st}$
$o=6$	$3^{rd}\ 2^{nd}\ 1^{st}$

Between time steps $k-1$ and k, there exist eight different types of crosses which could happen. Each cross type is composed of three boolean variables. These are used to codify whether or not a cross is declared between pairs of partitions. When the boolean variable is set to 1, a cross is declared between the corresponding pair of objects. For instance, one can adopt the following convention:

	Cross of partitions $1^{st}-2^{nd}$	Cross of partitions $1^{st}-3^{rd}$	Cross of partitions $2^{nd}-3^{rd}$
C1	0	0	0
C2	0	0	1
C3	1	0	0
C4	0	1	1
C5	1	1	0
C6	1	1	1
C7	1	0	1
C8	0	1	0

These cross-type codes can be used now for relative evaluation of the *order* at time step k, given the order at time step $k-1$.

	$o_k=1$	$o_k=2$	$o_k=3$	$o_k=4$	$o_k=5$	$o_k=6$
$o_{k-1}=1$	C1	C2	C3	C4	C5	C6
$o_{k-1}=2$	C2	C1	C7	C8	C6	C5
$o_{k-1}=3$	C3	C7	C1	C6	C8	C4
$o_{k-1}=4$	C4	C8	C6	C1	C7	C3
$o_{k-1}=5$	C5	C6	C8	C7	C1	C2
$o_{k-1}=6$	C6	C5	C4	C3	C2	C1

C. Simulation Results

The estimation performance of the CM method for a 3–1D objects scenario, using inequation (32) as the "cross detector", is illustrated in this subsection. Note that the validation method summarized in Section IV is based on evaluation of data association hypotheses. Therefore, Alg. 2 can be used right away to generate optimal LPEs and labeling probabilities in any arbitrary t–MD objects case. Fig. 9 illustrates the estimation performance of the CM tracker.

1) Discussion of Results: The results in Fig. 9 reveal remarkably accurate estimation performance of the CMT both in the computation of LPEs and labeling probabilities. This validates the CMT as a convenient solution to answer the questions in Section II for scenarios where an arbitrary number of objects move in one dimension.

The choice of the particular ground truth trajectories in Fig. 9 results in complete loss of labeling information (1/3! certainty for all LPEs). Although Fig. 9 illustrates this worst case scenario, it is apparent that the CMT accurately estimates labeling uncertain also in more favorable scenarios. For instance, scenarios where the objects remain closely-spaced for a shorter time and labeling certainty is lost only partially.

Disregarding the scenario, losing labeling information is a physical limitation inherent in closely-spaced object scenarios. Furthermore, once labeling certainty is lost, is mathematically not possible to recover it (assuming that the objects cannot be differentiated in measurements/maneuverability). In this context, all what can be expected from the tracker is that it captures the uncertainty produced by the combination scenario/sensor-limitations as accurately as possible. While regular TBD filters such as the one in [6] fail at doing so, the CMT reports successful results for the cases simulated so far.

VI. SECOND GENERALIZATION OF THE DEFINITION OF *cross*: FROM t–1D TO t–MD OBJECTS

Section III-B presented a generic DA-free decomposition of $p(\boldsymbol{s}_k|\mathbf{Z}_k)$ by introducing the (not yet defined) variable o_k. An analytical expression for the LPEs and labeling probabilities (dependent on the definition of o_k) was provided in equations (16) and (17). Another analytical derivation provided in Section V-A has proved that the relative calculation of o_k for the 2–1D objects case, based on inequation (32), leads to identical results than the absolute calculation of o_k based on equation (4).

Section V-B illustrated how the relative calculation of o_k [based on inequation (32)] can be extended seamlessly to cope with more than two objects moving in a one-dimensional space. This section covers the generalization of the relative calculation of o_k from 1D to MD objects. In practice, simulation experiments will be limited to cases where M is 2 and 3 to illustrate that the CMT

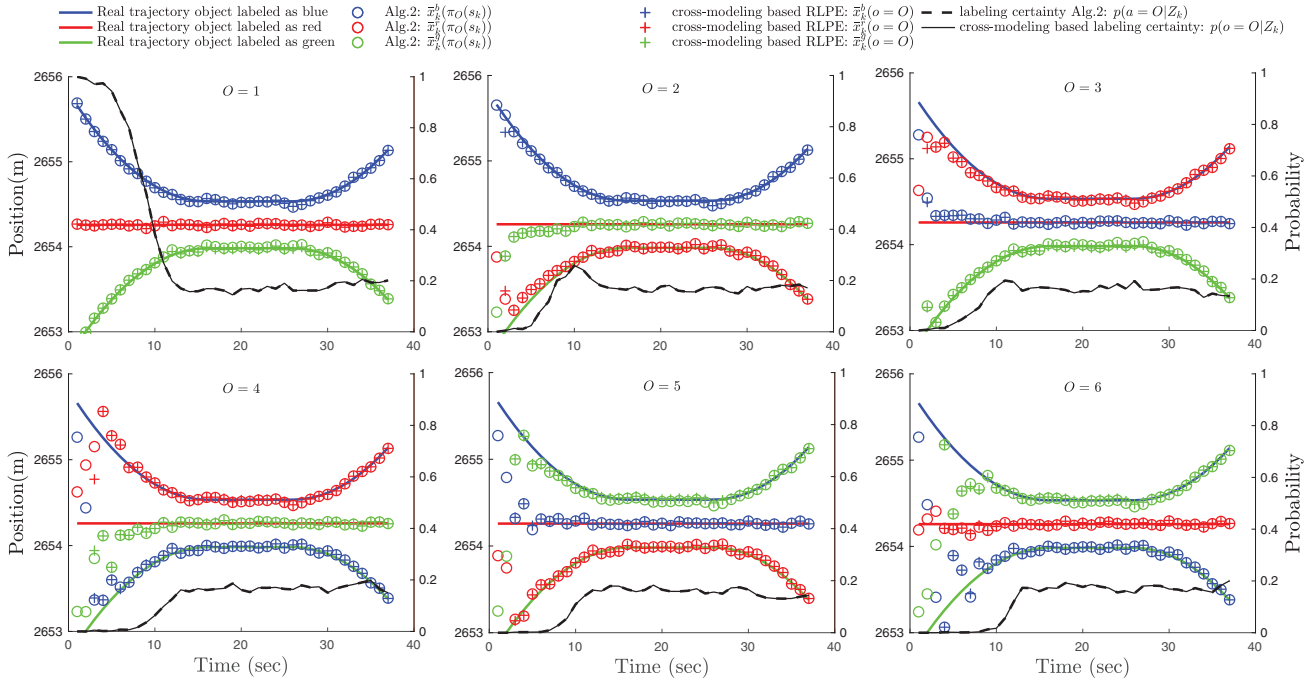

Fig. 9. Evaluation of estimation results provided from the clusters associated to all states of "order" in Table II.

can be used for tracking land/sea objects (2D) and air objects (3D).

The reader is referred to Appendix B at this point in order to understand the complexity of extending the definition of o_k in equation (4) to objects moving in 2 and 3 spacial dimensions.

A. Generalization of the *Cross* Detector for 2–2*D* Objects Settings

Inequation (32) does not extend straightforwardly from 2–1*D* to 2–2*D* objects scenarios as illustrated in Appendix B. However, the reason why inequation (32) works well for the 2–1*D* case can be found after analyzing the function K derived in Section V-A. Given the 2D points $\boldsymbol{s}'^p_{k-1}$ and $\boldsymbol{s}'^p_k$ (two objects in a 1D space), the function $K = 2(x^r_{k-1} - x^b_{k-1})(x^b_k - x^r_k)$ complies with a very particular condition:

$$K(\boldsymbol{s}'^p_{k-1}, \boldsymbol{s}'^p_k) = -K(\boldsymbol{s}'^p_{k-1}, \Pi(\boldsymbol{s}'^p_k)), \tag{33}$$

as $\boldsymbol{s}'^p_k$ and $\Pi(\boldsymbol{s}'^p_k)$ are crossed with respect to each other, K can be regarded as an odd function in the "order" of $\boldsymbol{s}'^p_k$. In other words, two different evaluations of K, using the current state of particle p and its permuted version are equal in absolute value but different in sign:

$$\begin{aligned} |K(\boldsymbol{s}'^p_{k-1}, \boldsymbol{s}'^p_k)| &= |K(\boldsymbol{s}'^p_{k-1}, \Pi(\boldsymbol{s}'^p_k))| \\ sgn(K(\boldsymbol{s}'^p_{k-1}, \boldsymbol{s}'^p_k)) &= sgn(-K(\boldsymbol{s}'^p_{k-1}, \Pi(\boldsymbol{s}'^p_k))). \end{aligned} \tag{34}$$

Additionally, as we already pointed out in Section V-A:

$$K(\boldsymbol{s}'^p_{k-1}, \boldsymbol{s}'^p_k) > 0 \quad \Leftrightarrow \quad \boldsymbol{s}'^p_{k-1}, \boldsymbol{s}'^p_k \textit{ are crossed}. \tag{35}$$

The condition $K(\boldsymbol{s}'^p_{k-1}, \boldsymbol{s}'^p_k) > 0$ and inequation (32) are equivalent "cross detectors" for the 2–1*D* case due to equation (29). Our problem formulation can be narrowed down to the following question: What is the 2–2*D* counterpart of the K function which can be applied to the two 4D points $\boldsymbol{s}'^p_{k-1}$ and $\boldsymbol{s}'^p_k$?

Let us consider an equivalent expression of K introducing the *norm* function, which we denote as K_{2-1D}:

$$\begin{aligned} K = K_{2-1D} = 2(norm(\boldsymbol{s}'^r_{k-1}) - norm(\boldsymbol{s}'^b_{k-1}))(norm(\boldsymbol{s}'^b_k) \\ -norm(\boldsymbol{s}'^r_k)). \end{aligned} \tag{36}$$

The desired function $K_{2-2D} : \mathbb{R}^8 \rightarrow \mathbb{R}$ can be found by considering the counterpart of K_{2-1D} for the 2–2*D* case:

$$\begin{aligned} K_{2-2D} = 2(norm(\boldsymbol{s}'^r_{k-1}) - norm(\boldsymbol{s}'^b_{k-1}))(norm(\boldsymbol{s}'^b_k) \\ -norm(\boldsymbol{s}'^r_k)). \end{aligned} \tag{37}$$

where now $\boldsymbol{s}'^p_k = [x^{p,b}_k\ y^{p,b}_k\ x^{p,r}_k\ y^{p,r}_k]^T$, $\boldsymbol{s}'^{p,r}_k = [x^{p,r}_k\ y^{p,r}_k]^T$ and $\boldsymbol{s}'^{p,b}_k = [x^{p,b}_k\ y^{p,b}_k]^T$. K_{2-2D} is indeed the odd function (in the "order" of $\boldsymbol{s}'_k$) which complies with the conditions in equations (33) and (35). Therefore, the extension of the definition of "cross" for the 2–2*D* objects case is:

$$K_{2-2D} > 0. \tag{38}$$

1) Simulations Results: The results provided by the CMT for the 2–2*D* objects case using inequation (38) as the "cross detector" are shown in Fig. 10.

B. Discussion of the Results

The results reveal remarkably accurate estimation performance of the CMT both in the computation of LPEs and labeling probabilities. This validates the CMT as a convenient solution to answer the questions in Section II for 2D objects. In fact, LPEs result in low

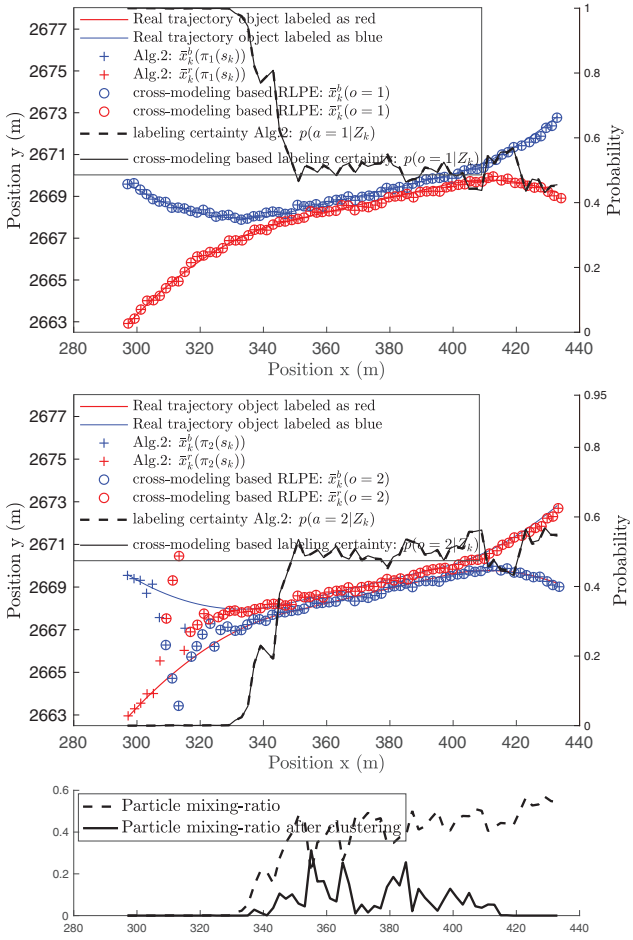

Fig. 10. Evaluation of estimation performance of the CM method when inequation (38) is used as the "cross detector." LPEs and labeling uncertainties are extracted from the clusters "order" 1 and 2, illustrated on top and middle figures. Alg. 2 is the performance evaluator algorithm. The figure at the bottom confirms that the "order detector" in inequation (38) is appropriate. In fact, the associated clustering method removes particle mixing within clusters after objects separation.

OSPA errors. This becomes possible even when extracting cost efficient MMSE [see equation (16)] point estimates thanks to the clustering method, which separates particles in different state of "order." These results support our argument that the design of the proper "cross detector" should produce a decomposition of $p(\boldsymbol{s}_k|\mathbf{Z}_k)$ where each component is unimodal. Also, very accurate estimation of labeling uncertainty is provided, which can be calculated by simply considering the proportion of particles within each order-dependent cluster [see equation (17)].

C. Generalization of the *Cross* Detector to 2–3*D* Objects Settings

The function $K_{2-3D} : \mathbb{R}^{12} \rightarrow \mathbb{R}$ is the counterpart of K_{2-1D} for the 2–3*D* objects case:

$$K_{2-3D} = 2(norm(\boldsymbol{s}'^r_{k-1}) - norm(\boldsymbol{s}'^b_{k-1}))(norm(\boldsymbol{s}'^b_k) - norm(\boldsymbol{s}'^r_k)), \quad (39)$$

where now $\boldsymbol{s}'^p_k = [x^{p,b}_k\ y^{p,b}_k\ z^{p,b}_k\ x^{p,r}_k\ y^{p,r}_k\ z^{p,b}_k]^T$. As $\boldsymbol{s}'^p_k$ and $\Pi(\boldsymbol{s}'^p_k)$ are in different states of "order," K_{2-3D} is also and odd function (in the "order" of $\boldsymbol{s}'^p_k$) which complies with the conditions in equations (33) and (35). The evaluations of the current state and its permuted version are equal in absolute value but different in sign. Therefore, the exact same definition for the "cross detector" from K_{2-1D} and K_{2-2D} cases can be used in the K_{2-3D} case:

$$K_{2-3D} > 0. \quad (40)$$

1) Simulations Results: The results provided by the CM method for the 2–3*D* objects case using inequation (40) as the "cross detector" are shown in Figs. 11 and 12.

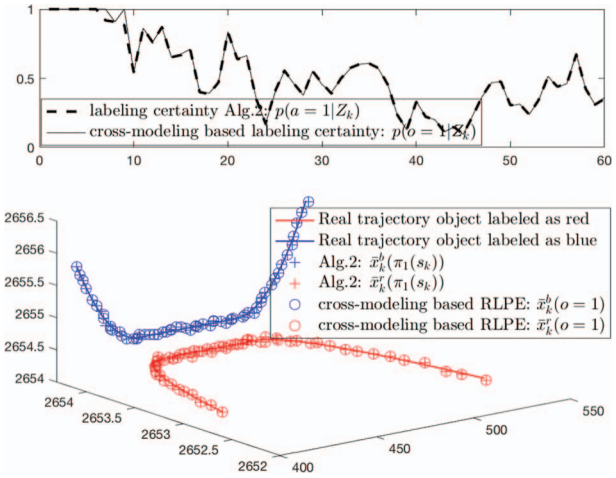

Fig. 11. Evaluation of estimation performance of the CM method when inequation (40) is used as the "order switch" detector. Labeled point estimates are extracted from the cluster "order" 1. Alg. 2 is the performance evaluator algorithm.

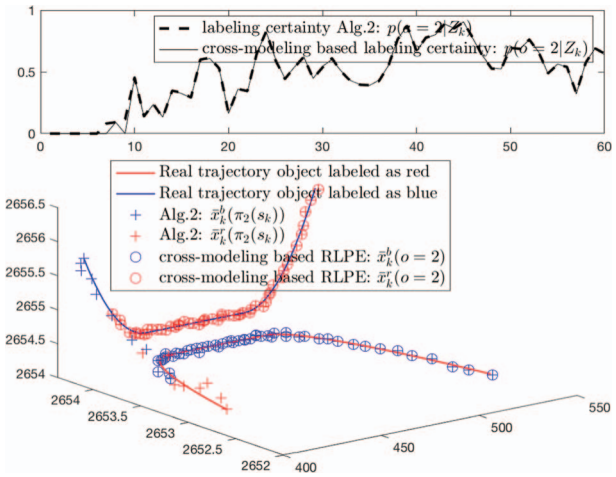

Fig. 12. Evaluation of estimation performance of the CM method when inequation (40) is used as the "cross detector." Labeled point estimates are extracted from the cluster "order" 2. Alg. 2 is the performance evaluator algorithm.

D. Discussion of the Results

The results reveal remarkably accurate estimation performance of the CMT both in the computation of

LPEs and labeling probabilities. This validates the CMT as a convenient solution to answer the questions in Section II also for 3D objects.

VII. CONCLUSIONS

Cross Modeling Tracking has been presented as a DA-free solution to the MOT problem. DA-free solutions are specially relevant in the TBD context, where advantages concerning tracking of low SNR and closely-spaced objects have been reported in previous literature. The main contribution of the paper is the non-trivial generalization of the idea in [17, Section IV] from the 2–1D objects case to the t–MD objects cases.

The underlying problem to solve the MOT problem in TBD has been formulated as: how to decompose a DA-free Bayes posterior so that labeling uncertainty can be characterized. The reviewed method in [17, Section IV] provides an answer based on modeling crosses between objects, but it is only suitable in the 2–1D objects case. A generic formulation of the desired decomposition for the t–MD case is provided. Furthermore, the generalized definition of cross-between-objects has been derived from a meaningful interpretation of the problem in the low dimensional setting.

The paper also revisits the method in [18] and uses it to generate optimal references in order to evaluate estimation performance of the CMT. Simulation results involving challenging closely-spaced objects scenarios have been provided. The results illustrate that the CMT is usable in the general t–MD objects case under the assumption that t is known and constant. Therefore, the proposed solution extends the state-of-the-art of TBD MOT. For the first time in literature, characterization of labeling uncertainty with validated estimation performance and efficient scalability has been provided for seamless use in TBD context.

As for future work, the formulation of the CMT within the RFS framework will be investigated in order to add cardinality estimation capabilities. This is required for the CMT to be declared as a solution for the complete MOT problem, where the assumption of known and constant number of objects does not hold. Additionally, studying the use of the CMT in the context of DBT may lead to interesting advantages. This may be specially the case when comparing with DBT methods in scenarios where DA needs to account for large number of non-negligible hypotheses.

APPENDIX A RELATION BETWEEN THE DATA ASSOCIATION PROBLEM AND THE LABELING PROBLEM

Definitions:

- DA defines hypotheses matching detections and labels.
- Labeling association defines hypotheses matching point estimates and labels.

Applicability:

- DA applies before update.
- Labeling association applies after update and point estimate extraction.

The interesting problem from the application point of view is the labeling problem. The purpose of this appendix is illustrating that:

- DBT trackers only tackle the DA problem. However, once the DA problem is solved, the solution of the labeling problem follows right away: one only needs to perform association dependent updates and extract (labeled) point estimates.

Let us take the following considerations in order to prove that once DA is solved, the solution to the labeling problem follows right away:

- In DBT context, let us consider:
  - Perfect detectability, no false detections.
  - No merged measurements.
  - The measurements do not provide any info about label.

Let us define $\boldsymbol{\varkappa}_k$ as the vector of detections at time step k with explicit indication of correct DA: $\boldsymbol{\varkappa}_k = [\boldsymbol{p}_1, \boldsymbol{p}_2, ..., \boldsymbol{p}_t]^T$. The vector $\boldsymbol{\omega} = [\pi_1, \pi_2, ..., \pi_{t!}]^T$ contains the functions to perform all possible permutations of t elements. The tracker cannot access $\boldsymbol{\varkappa}_k$ but an unlabeled version of it, which we denote as $\boldsymbol{z}_k$.

The DBT measurement $\boldsymbol{z}_k$ is a set since different ways of ordering detections define the same measurement. Nevertheless, one can formulate $\boldsymbol{z}_k$ as a vector, $\boldsymbol{z}_k = [\boldsymbol{d}_1, \boldsymbol{d}_2, ..., \boldsymbol{d}_t]^T$. Note that the subscripts in $\boldsymbol{\varkappa}_k$ are labels, the subscripts in $\boldsymbol{z}_k$ only define the particular order in which detections are collocated, as this order is random:

$$P(\boldsymbol{z}_k = \pi_m(\boldsymbol{\varkappa}_k)) = P(\boldsymbol{z}_k = \pi_n(\boldsymbol{\varkappa}_k)) \quad \forall\{m, n\} : \{\pi_m, \pi_n\} \in \boldsymbol{\omega}. \tag{41}$$

Let us consider the state vector $\boldsymbol{s}_k$, where the individual states of t objects are staked with explicit indication of labels: $\boldsymbol{s}_k = [\boldsymbol{s}_k^1, \boldsymbol{s}_k^2, ..., \boldsymbol{s}_k^t]^T$. Solving the DA problem requires: generation of DA hypotheses and evaluation of the DA hypotheses. Let us use $\boldsymbol{h}_k$ to note the set of generated DA hypotheses: $\boldsymbol{h}_k = \{(\boldsymbol{a_1}, \boldsymbol{a_2}, ..., \boldsymbol{a_{t!}})\}$, where $\boldsymbol{a_m} = \pi_m(\boldsymbol{z}_k)$, for m =1, 2, .., t!. Note that the subscripts in the vector $\boldsymbol{a_m}$ are not labels, the labels are implicit in the order of $\boldsymbol{a_m}$. For illustrative purposes, consider there are two objects and $\boldsymbol{a_1} = [\boldsymbol{d^2}, \boldsymbol{d^1}]^T$: this means that $\boldsymbol{a_1}$ hypothesizes that the detection which came in second position in $\boldsymbol{z}_k$ was produced by target labeled as 1 and the one which came in first position was produced by the target labeled as 2.

Given the model for the likelihood of the measurements conditioned on the state $l(\boldsymbol{z}_k|\boldsymbol{s}_k)$, a DA dependent

decomposition of $p(\boldsymbol{s}_k|\boldsymbol{Z}_k)$ can be formulated as:

$$p(\boldsymbol{s}_k|\boldsymbol{Z}_k) \propto \sum_{m=1}^{t!} l(\pi_m(\boldsymbol{z}_k)|\boldsymbol{s}_k)p(\boldsymbol{s}_k|\boldsymbol{Z}_{k-1}). \tag{42}$$

From equation (42), one can conclude that in DBT an analytical decomposition relevant for labeling characterization follows from solving the DA problem. In fact, each component in the sum directly relates one DA hypotheses $\pi_m(\boldsymbol{z}_k)$ with its association-dependent posterior $l(\pi_m(\boldsymbol{z}_k)|\boldsymbol{s}_k)p(\boldsymbol{s}_k|\boldsymbol{Z}_{k-1})$. Furthermore, extraction of sufficient statistics from each component in the sum, by minimizing the MMSE, provides a labeled point estimate. Note that a labeled point estimate explicitly hypothesizes one particular association between point estimates and labels. This trivial derivation demonstrates that once DA is solved, the solution of the labeling problem follows right away.

Remarks:

- The analytical evaluation of labeling association hypotheses has a one-to-one relation to the evaluation of DA hypotheses. In particular, the certainty associated to the labeled point estimate extracted from $l(\pi_m(\boldsymbol{z}_k)|\boldsymbol{s}_k)p(\boldsymbol{s}_k|\boldsymbol{Z}_{k-1})$ is:

$$p(\pi_m(\boldsymbol{z}_k)|\boldsymbol{Z}_k) = \frac{\int l(\pi_m(\boldsymbol{z}_k)|\boldsymbol{s}_k)p(\boldsymbol{s}_k|\boldsymbol{Z}_{k-1})d\boldsymbol{s}_k}{\sum_{m=1}^{t!}\int l(\pi_m(\boldsymbol{z}_k)|\boldsymbol{s}_k)p(\boldsymbol{s}_k|\boldsymbol{Z}_{k-1})d\boldsymbol{s}_k}. \tag{43}$$

- Under the assumption that $p(\boldsymbol{s}_k|\boldsymbol{Z}_{k-1})$ can be formulated as one single density $\forall k$, equation (42) does not run into combinatorial explosion over time.
- This analytical derivation is the base of the optimal reference that will be used to evaluate the CMT proposed as the main contribution of this paper.
- Note that the evaluations of $l(\pi_m(\boldsymbol{z}_k)|\boldsymbol{s}_k)$ and $l(\boldsymbol{z}_k|\pi_m(\boldsymbol{s}_k))$ are equivalent. Therefore, equation (42) can be rewritten as:

$$p(\boldsymbol{s}_k|\boldsymbol{Z}_k) \propto \sum_{m=1}^{t!} l(\boldsymbol{z}_k|\pi_m(\boldsymbol{s}_k))p(\boldsymbol{s}_k|\boldsymbol{Z}_{k-1}). \tag{44}$$

APPENDIX B NAIVE GENERALIZATION OF o_k

A naive extension of the definition of "cross" from 2–1D to 2–2D settings will be presented in this appendix. This is not only to illustrate the complexity of the problem but also to familiarize the reader with some consistency checks that the correct extension of "cross" should comply with.

The naive attempt presented in this appendix considers that inequation (32) is the "cross detector" for the 2–2D objects case. After all, a point can be evaluated by the $l2-norm$ function disregarding the dimensionality of the point. Only two formal modifications need to be accounted for when extending inequation (32) from 2–1D to 2–2D settings. First, the $l2-norm$ calculation for the 2–2D objects case becomes:

$$norm(\boldsymbol{s}'_k - \boldsymbol{s}'_{k-1}) = \sqrt{(x^r_k - x^r_{k-1})^2 + (x^b_k - x^b_{k-1})^2 + (y^r_k - y^r_{k-1})^2 + (y^b_k - y^b_{k-1})^2}, \tag{45}$$

where now $\boldsymbol{s}'^{p}_k = [x^{p,b}_k\ y^{p,b}_k\ x^{p,r}_k\ y^{p,r}_k]^T$. Second, the permutation matrix Π for the 2–2D objects case becomes:

$$\Pi = \begin{pmatrix} 0 & 0 & 1 & 0 \\ 0 & 0 & 0 & 1 \\ 1 & 0 & 0 & 0 \\ 0 & 1 & 0 & 0 \end{pmatrix}. \tag{46}$$

Given these modifications, the results provided by the CMT for the 2–2D objects case are shown in Fig. 13.

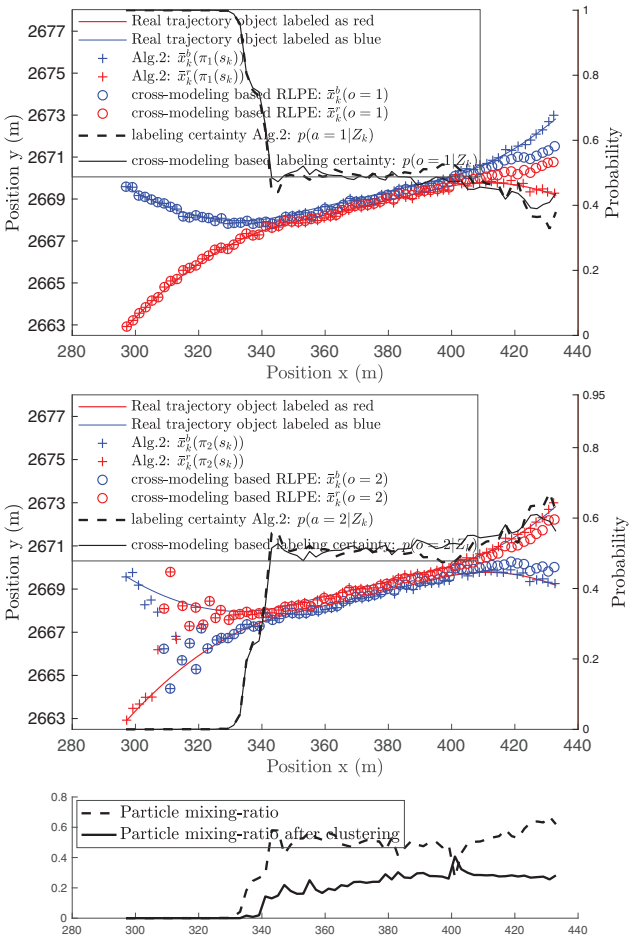

Fig. 13. Evaluation of estimation performance of the CM method using a naive 2–2D "cross" detector. Alg. 2 generates the optimal references.

The results reveal degraded estimation performance of the CMT both in the computation of LPEs and labeling probabilities. In fact, LPEs result in high OSPA errors (specially after objects separation) due to the well known "track coalescence" effect. This undesired effect

is expected if MMSE point estimates are extracted from multimodal densities when labeling uncertainty characterization is not appropriately accounted for.

One can conclude that this attempt to generalize the definition of "cross" is naive. In fact, the use of inequation (32) as the "cross detector" does not remove particle mixing inside each cluster after objects separation. This is illustrated at the bottom part of Fig. 13, where the particle mixing-ratio using CMT clustering, calculated as the ratio between the number of "mixed particles" and the total number of particles, does not drop to zero after target separation.

REFERENCES

[1] E. H. Aoki, P. K. Mandal, L. Svensson, Y. Boers, and A. Bagchi "Labeling uncertainty in multitarget tracking," *IEEE Trans. Aerosp. Electron. Syst.*, vol. 52, no. 3, pp. 1006–1020, Jun. 2016.

[2] Y. Bar-Shalom, X. Rong Li, and T. Kirubarajan *Estimation with Applications to Tracking and Navigation: Theory, Algorithms and Software*. Canada: Wiley, 2001.

[3] S. Blackman and R. Popoli *Design and Analysis of Modern Tracking Systems*. Norwood, MA: Artech House, 1999.

[4] H. Blom and E. Bloem "Permutation invariance in Bayesian estimation of two targets that maneuver in and out formation flight," in *Proc. 12th Int. Conf. Inf. Fusion*, Seattle, 2009, pp. 1296–1303

[5] H. Blom, E. Bloem, Y. Boers, and H. Driessen "Tracking closely spaced targets: Bayes outperformed by an approximation?," in *Proc. 11th Int. Conf. Inf. Fusion*, Cologne, 2008, pp. 1–8.

[6] Y. Boers and J. N. Driessen "Multitarget particle filter track before detect application," *IEE Proc. Radar Sonar Navig.*, vol. 151, no. 6, pp. 351–357, Dec. 2004.

[7] Y. Boers and H. Driessen "The mixed labeling problem in multi target particle filtering," in *Proc. 10th Int. Conf. Inf. Fusion*, Quebec, 2007, pp. 1–7.

[8] Y. Boers, E. Sviestins, and H. Driessen "Mixed labelling in multitarget particle filtering," *IEEE Trans. Aerosp. Electron. Syst.*, vol. 46, no. 2, pp. 792–802, Apr. 2010.

[9] D. F. Crouse, P. Willett, and Y. Bar-Shalom "Generalizations of Blom and Bloem's PDF decomposition for permutation-invariant estimation," *Proc. 2011 IEEE Int. Conf. Acoust. Speech Signal Process.*, 2011, pp. 3840–3843

[10] D. F. Crouse, P. Willett, and Y. Bar-Shalom "Developing a real-time track display that operators do not hate," in *IEEE Trans. Signal Process.*, vol. 59, no. 7, pp. 3441–3447, Jul. 2011.

[11] D. F. Crouse, P. Willett, L. Svensson, D. Svensson, and M. Guerriero "The Set MHT," in *14th Int. Conf. Inf. Fusion*, Chicago, IL, 2011, pp. 1–8.

[12] M. Ekman, E. Sviestins, L. Sjoberg, Y. Boers, and H. Driessen "Particle filters for tracking closely spaced targets," in *Proc. 10th Int. Conf. Inf. Fusion*, Quebec, 2007, pp. 1–8.

[13] T. Fortmann, Y. Bar-Shalom, and M. Scheffe "Sonar tracking of multiple targets using joint probabilistic data association," *IEEE J. Ocean. Eng.*, vol. 8, no. 3, pp. 173–184, Jul. 1983.

[14] A. F. García-Fernández "Track-before-detect labeled multi-bernoulli particle filter with label switching," *IEEE Trans. Aerosp. Electron. Syst.*, vol. 52, no. 5, pp. 2123–2138, Oct. 2016.

[15] A. F. García-Fernández, M. Morelande, and J. Grajal "Particle filter for extracting target label information when targets move in close proximity," in *Proc. 14th Int. Conf. Inf. Fusion*, Chicago, 2011, pp. 1–8.

[16] A. F. García-Fernández, L. Svensson, and M. R. Morelande "Multiple target tracking based on sets of trajectories," *IEEE Trans. Aerosp. Electron. Syst.* vol. 56, no. 3, pp. 1685–1707, Jun. 2020.

[17] C. M. Leon, H. Driessen, and P. K. Mandal "Efficient characterization of labeling uncertainty in closely-spaced targets tracking," in *Proc. 19th Int. Conf. Inf. Fusion*, Heidelberg, 2016, pp. 449–456.

[18] C. M. Leon and H. Driessen "Evaluation of labeling uncertainty in multiple target tracking with track-before-detect radars," in *Proc. 22nd Int. Conf. Inf. Fusion*, Ottawa, 2019, pp. 1–8.

[19] R. Mahler "Multitarget Bayes filtering via first-order multitarget moments," *IEEE Trans. Aerosp. Electron. Syst.*, vol. 39, no. 4, pp. 1152–1178, Oct. 2003.

[20] M. R. Morelande and A. Zhang "Uniform sampling for multiple target tracking," in *Proc. 14th Int. Conf. Inf. Fusion*, Chicago, 2011, pp. 1–7.

[21] D. Reid "An algorithm for tracking multiple targets," *IEEE Trans. Automat. Contr.*, vol. 24, no. 6, pp. 843–854, 1979.

[22] B. Ristic, S. Arulampalam, and N. Gordon *Beyond the Kalman Filter: Particle Filters for Tracking Applications*. Norwood, MA, USA: Artech House, 2004.

[23] L. Svensson and M. Morelande "Target tracking based on estimation of sets of trajectories," in *Proc. 17th Int. Conf. Inf. Fusion*, Salamanca, 2014, pp. 1–8.

[24] Y. Xia, L. Svensson, A. F. García-Fernández, K. Granström, and J. L. Williams "Backward simulation for sets of trajectories," in *Proc. 23rd Int. Conf. Inf. Fusion*, virtual, 2020, pp. 1–8.

Carlos Moreno Leon received his MSc in Telecommunications Engineering in 2013 from the University of Alcalá (UAH) in Madrid. From 2012 to 2014 he was employed with the Polytechnic University of Madrid (UPM) as a research assistant in the Signal, Systems and Radiocommunications department. From 2014 to 2017 he held a European Commission Marie Curie research fellowship while working at Thales Nederland BV. Since 2017 he is with the Cognitive Radar department in the German Fraunhofer Institute for High Frequency Physics and Radar Techniques (FHR). Parallel to his work at Fraunhofer FHR, he is pursuing a PhD at TU-Delft since November 2017 (in the Microwave Signals Sensor and Systems group). He has been involved in several international research and development projects in the area of signal/data processing with applications in Wireless Sensor Networks and Radar Technology both within civilian and military contexts.

Hans Driessen obtained the MSc and PhD degree in 1987 and 1992, respectively, both from the department of Electrical Engineering at the TU-Delft. Since then he has been employed with Thales Nederland BV. He has been and is still involved in various (international) research projects and radar development programs in the area of signal/data processing and radar management. Since January 2015, he additionally holds a part-time position as associate professor at the EEMCS faculty in the Microwave Signals Sensor and Systems group in the field of radar systems; waveforms and processing. His interest is in the practical application of detection, estimation, information and control theory to various problems in sensor systems.

Alexander Yarovoy (FIEEE'2015) graduated from the Kharkov State University, Ukraine, in 1984 with the Diploma with honor in radiophysics and electronics. He received the Candidate Phys. & Math. Sci. and Doctor Phys. & Math. Sci. degrees in radiophysics in 1987 and 1994, respectively. In 1987 he joined the Department of Radiophysics at the Kharkov State University as a Researcher and became a Full Professor there in 1997. From September 1994 through 1996 he was with Technical University of Ilmenau, Germany as a Visiting Researcher. Since 1999 he is with the Delft University of Technology, the Netherlands. Since 2009 he leads there a chair of Microwave Sensing, Systems and Signals. His main research interests are in high-resolution radar, microwave imaging and applied electromagnetics (in particular, UWB antennas). He has authored and co-authored more than 450 scientific or technical papers, six patents and fourteen book chapters. He is the recipient of the European Microwave Week Radar Award for the paper that best advances the state-of-the-art in radar technology in 2001 (together with L.P. Ligthart and P. van Genderen) and in 2012 (together with T. Savelyev). In 2010 together with D. Caratelli Prof. Yarovoy got the best paper award of the Applied Computational Electromagnetic Society (ACES). Prof. Yarovoy served as the General TPC chair of the 2020 European Microwave Week (EuMW'20), as the Chair and TPC chair of the 5th European Radar Conference (EuRAD'08), as well as the Secretary of the 1st European Radar Conference (EuRAD'04). He served also as the co-chair and TPC chair of the Xth International Conference on GPR (GPR2004). He served as an Associated Editor of the *International Journal of Microwave and Wireless Technologies* from 2011 till 2018 and as a Guest Editor of five special issues of the IEEE Transactions and other journals. In the period 2008-2017 Prof. Yarovoy served as Director of the European Microwave Association (EuMA).